Preprints of the 21st IFAC World Congress (Virtual)
Berlin, Germany, July 12-17, 2020

Automatic adjustment method for cascade control system based on iterative setting of stability-margin criterion circle

Ryohei Kitayoshi * **Hiroshi Fujimoto** **

* *Tsukuba Research Laboratory Corporate Technology Division YASKAWA Electric Corporation, 9-10 Tokodai 5 Chome, Tsukuba, Ibaraki, 300-2635 Japan (e-mail:kitayoshi.ryohei18@ae.k.u-tokyo.ac.jp).*
** *University of Tokyo, 5-1-5 Kashiwanoha, Kashiwa, Chiba, 277-8561, Japan (e-mail: fujimoto@k.u-tokyo.ac.jp)*

Abstract: Demand for servo motors has increased in recent years as rising factory automation. With the increase in demand, controller adjustment work before the start of the production line has also been growing.
Accordingly, we propose a novel automatic adjustment method that enables us to optimize controller parameters and controller structure and to overcome the conservativeness of the circle condition in the cascade control system. Previously, the performance of the controller based on the circle condition could be conservative. Therefore, we solve this problem by setting a criterion circle designed by stability margin iteratively and adjusting controller parameters and controller structure until stability margin is close enough to design value. The effectiveness of the proposed method is verified by the experiment with the high precision positioning device.

Keywords: Adjustment method of controller, Cascade position control system, Stability-margin criterion circle, Bundle method

1. INTRODUCTION

Recently, demand for servo motor has been increasing because the need for factory automation has been rising in the world. This tendency is particularly remarkable in the field of precise positioning devices such as semiconductor manufacturing equipment and liquid crystal exposure equipment. According to the growth of demand, there has also been increasing customer's request to develop easy-to-use applications that can shorten the adjusting time before the operation of the production line. To satisfy the customer's request, the development of the automatic adjustment method of a servo motor is a significant challenge in the industry.

For achieving this task, a lot of studies have been conducted in recent years. Apkarian and Noll (2006) and Apkarian and Noll (2017) proposed the adjustment method of fixed structure controller parameters based on the frequency response data of a plant. Maeda et al. (2018) achieved the design of the cascade structure FB controller by a combination of the sequential quadratic programming (SQP) and genetic algorithm (GA). Nakamura et al. (2016) and Ohnishi (2019) proposed a fixed-order controller design method maximizing control bandwidth based on the frequency responses with Concave-Convex Procedure (CCCP) Yuille and Rangarajan (2003). Seki et al. (2018) illustrated the design method of a dual loop controller based on the loop-shaping approach considering system stability and vibration suppression characteristics. Besides the above, adjustment methods of the parameters of the fixed structure controller Karimi et al. (2008). Oomen (2018) also proposed control design methods and system identification methods based on frequency response data.

Fig. 1. Servo motors and servo packs released by YASKAWA Electric Corporation

In previous researches, it is possible to optimize parameters of the controller on the premise that structure of controller is fixed. However, it is impossible to optimize the structure of the controller. Therefore, Kitayoshi and Fujimoto (2019) proposed the automatic adjustment method, that enables us to optimize the structure of the controller. Nevertheless, there is a problem that the stability margin becomes larger than a design value, and the performance of the controller is conservative.

Therefore, we propose a new adjusting method that can obtain the gain margin according to the design value while optimizing the controller structure and parameters. The

Copyright lies with the authors

conservativeness is solved by setting a criterion circle based on stability margin iteratively and adjusting controller parameters and controller structure until the stability margin is close enough to design value. This iterative setting of the criterion circle is the originality of our study. The criterion circle is called "stability-margin criterion circle " in this study.

This study is organized as follows. Firstly, in Section 2, the cascade position control system as an adjustment target is explained. In Section 3, we describe the detail of our proposed method. In Section 4, we explain a high precision positioning device. In Sections 5 and 6, the results of the simulation and experiment of the proposed method are explained. Finally, in Section 7, conclusions of this study are explained.

2. CASCADE POSITION CONTROL SYSTEM AS AN ADJUSTMENT TARGET

In this study, the control system assumes a cascade position control system shown in Fig.2. This is because the cascade position control system is one of the most common controllers of servo-motors for high precision position control. The cascade position control system consists of P-PI controller and Basis filter. $P(s)$ denotes a frequency characteristic of a plant. X_{ref} and X_m represent a position reference and a motor-side position, respectively.

2.1 P-PI controller

P-PI controller is a basic structure in the cascade position control system. Therefore, the structure is fixed, and only parameters, which are K_p, K_v, and K_i, are adjusted. Initial values of the parameters and adjustment range are shown in Table.1. Initial values were set to the values that poles of the transfer function from X_{ref} to X_m were four roots if the plant is a rigid body. $D(s)$ denotes a pseudo - differentiator and its time constant value is fixed, which is 400 μs.

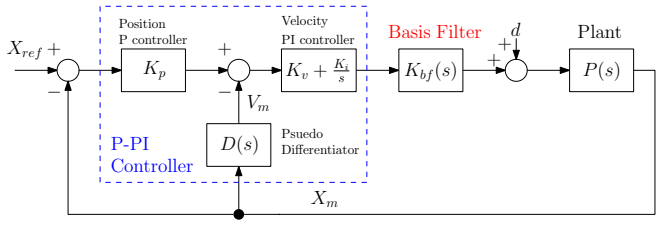

Fig. 2. Block diagram of position control system to be adjusted

Table 1. Tunable parameters of the controller ("Init" means an initial value for optimization)

Sym	Parameter	Min	Max	Init	Unit
K_p	Position P gain	0	2000	10	rad/s
K_v	Velocity P gain	0	2000	62.8	rad/s
K_i	Velocity I gain	0	2000	251	1/s
ω_{fi}	Frequency of notch	0	1250	625	Hz
ζ_{d1i}	Damping ratio	0	1	0.5	rad/s
α_i	Depth of notch	0	1	0.5	-
$\omega_{\ell i}$	Frequency of phase lead	0	1250	625	Hz
β_i	Coefficient of phase lead	0.85	1	0.90	-

2.2 Basis-filter

Basis filter is multiple filters that adjust the structure of the control system. By changing the number and types of the filters used in Basis filter, the structure of the controller is adjusted. In this study, Basis filter shown in (1) and (2) is constituted of notch filters and phase-lead compensations. There are two aims to provide Basis filter in this configuration.
Aim1: To be able to adjust gain and phase freely in the adjustment range.
Aim2: To prevent the unnecessary increase of the controller order.
The aim1 means that notch filters eliminate the peak gain caused by the resonance characteristics of the plant, and the phase-lead compensations compensate phase-lag caused by dead time and notch filters. The aim2 means that pole-zero cancellation occurs in the notch filter term or the phase-lead compensation, and the controller order is reduced. The control system with too high order is undesirable because a lot of difference calculations are likely to excite sensor noise and high frequency components of the position reference.

$$K_{bf}(s) = \prod_{i=1}^{m} G_{bfi}(s) \tag{1}$$

$$G_{bfi}(s) = \frac{s^2 + 2\alpha_i\zeta_{di}\omega_f s + \omega_f^2}{s^2 + 2\zeta_{di}\omega_f s + \omega_f^2} \cdot \frac{s + \omega_\ell}{\beta_i s + \omega_\ell} \tag{2}$$

2.3 Disturbance suppression characteristics

We focus on the disturbance suppression characteristics of the cascade position control system. To suppress the input disturbance d, it is important to lower the gain of the sensitivity function $S(s)$ in (3). The sensitivity function $S(s)$ is expressed by the open loop function $L(s)$ in (4).

$$S(s) = \frac{1}{L(s) + 1} \tag{3}$$

$$L(s) = \Big(K_p + D(s)\Big)\Big(K_v + \frac{K_i}{s}\Big)K_{bf}(s)P(s) \tag{4}$$

3. PROPOSED ADJUSTMENT METHOD

We propose an automatic adjustment method that enables us to optimize controller parameters and controller structure and to overcome the conservativeness of the circle condition Zames (1966), Molander and Willems (1980). The adjustment flow shown in Fig. 3 consists of two parts: one is adjustment of controller structure and adjustment of the stability-margin criterion circle.
The initial parameters of the controller were set in Table.1. Number of Basis filter is one, that is, $m = 1$.

3.1 Adjustment of the controller structure

Adjustment of the controller structure is achieved by optimization of controller parameters and increase number of Basis filter.

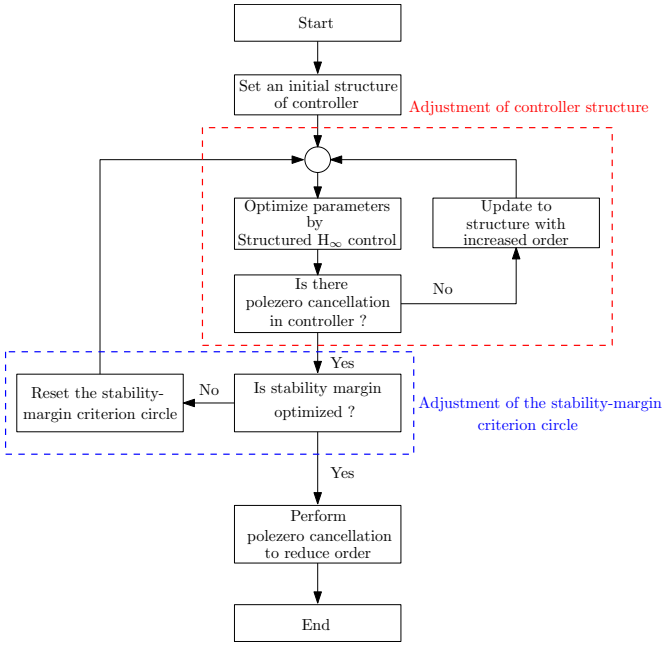

Fig. 3. Flowchart of the proposed method

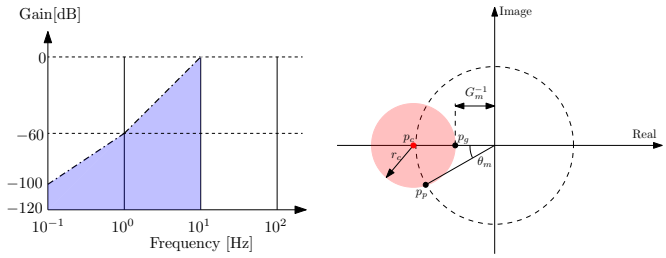

(i) Target specification of Sensitivity function

(ii) Constraint condition of stability

Fig. 4. Target specification and constraint conditions

3.2 Optimization calculation of controller parameters

Optimization performs based on one target specification and two constraint conditions.

Target specification: Slope of sensitivity function is smaller than -60 dB/dec from 1.0 Hz to 10.0 Hz and smaller than -40 dB/dec from 0.1 Hz to 1.0 Hz in Fig.4-(i)
Constraint1: Gain margin: 6 dB, Phase margin: 30 deg
Constraint2: All parameters are non-negative.

From above the specification and conditions, we optimize parameters shown in (5) $\sim$ (8). (7) expresses the constraint1, and a red circle in Fig.4-(ii) is designed by the gain margin and phase margin. This red circle is called "stability-margin criterion circle" in this study. Optimization method is bundle method [Do and Artieres (2012)]. Bundle method is implemented as MATLAB function "systune" [Gahinet and Apkarian (2011)].

$$\arg\min_{\rho} \delta \tag{5}$$

$$||W_s(\omega)S(\omega,\rho)|| \leq \delta \tag{6}$$

$$|p_c - L(\omega,\rho)| \geq r_c \tag{7}$$

$$\rho \geq 0 \tag{8}$$

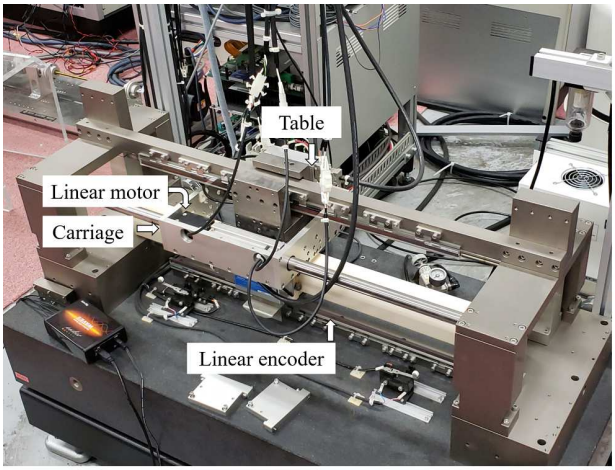

Fig. 5. Overview of the single axis positioning device

3.3 Adjustment of stability-margin criterion circle

After the adjustment of controller structure, if both the gain margin and phase margin are sufficiently larger than the stability constraint value, we improve disturbance suppression performance by resetting the stability-margin criterion circle and performing optimization calculation. For the resetting the stability-margin criterion circle, we calculate a new gain margin from (9), and set it as a constraint condition when performing optimization of the controller parameters. G_{des} expresses the gain margin which we want to adjust, and this value is 6 dB now. $G_m(n)$ represents the gain margin obtained by the n-th optimization. $G_{obj}(n)$ expresses the gain margin set as the constraint condition at the n-th optimization.

$$G_{obj}(n+1) = \frac{G_{des}}{G_m(n)} \times G_{obj}(n) \tag{9}$$

4. HIGH PRECISION POSITIONING DEVICE

The plant of the position control system $P(s)$ is a single axis high precision positioning device shown in Fig.5. In our laboratory, researches on high speed and high precision motion control [Fujimoto and Sakata (2014)] have been conducted with this device.

4.1 Mechanical configuration

This positioning device mainly consists of four parts: a linear motor, a carriage, a table and two linear encoders. The linear motor drives the carriage directly. Between the carriage and the table, a leaf spring is connected. The table is driven by the repulsive force of the leaf spring. The linear encoders can measure both of the position of the carriage and the table with 1 nano meter resolution. The control system is a semi-closed loop system which feeds back the position of the carriage : X_m and the velocity of the carriage: V_m shown in Fig.2.

4.2 Frequency characteristic of the device

The frequency characteristic of the positioning device is illustrated in Fig.6, and the mathematical model of the

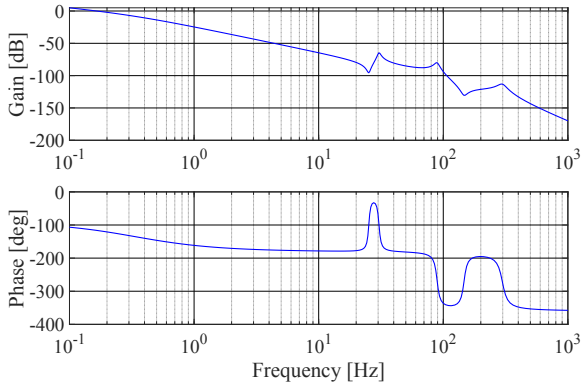

Fig. 6. Bode diagram of the plant (Input : current reference, Output : position of the carriage)

plant is expressed in (10). This Bode diagram shows the linear characteristic from the current reference to the position of the carriage. As can be seen in Fig.6, this device has multiple vibration modes. The first vibration mode has an antiresonance frequency at 27 Hz and a resonance frequency at 35 Hz. The second vibration mode has an antiresonance frequency at 140 Hz and a resonance frequency at 89 Hz. The third vibration mode has a resonance frequency at 300 Hz.
These vibration modes make it difficult to adjust parameters and structure of the controller. Especially, the resonance of the second vibration mode makes the position control system unstable when setting the parameters of the P-PI controller to high gain . Therefore, it is necessary to suppress the influence of the resonance by adjusting the controller.

$$P(s) = \frac{\sum_{k=0}^{4} a_k \cdot s^k}{s^8 + \sum_{l=1}^{7} b_l s^l} \tag{10}$$

$$\begin{aligned}
&a_4 = 4.6 \cdot 10^6 && a_3 = 4.2 \cdot 10^8 && a_2 = 4.0 \cdot 10^{12} \\
&a_1 = 4.1 \cdot 10^{13} && a_0 = 9.8 \cdot 10^{16} && \\
&b_7 = 320 && b_6 = 3.0 \cdot 10^{12} && b_5 = 3.0 \cdot 10^8 \\
&b_4 = 1.2 \cdot 10^{12} && b_3 = 2.3 \cdot 10^{13} && b_2 = 4.0 \cdot 10^{16} \\
&b_1 = 8.5 \cdot 10^{16} &&&&
\end{aligned}$$

5. SIMULATION FOR VALIDATION

We performed a simulation to confirm the validation of the proposed method. Firstly, the adjustment result of the controller structure is illustrated. Secondly, the adjustment of the stability margin is explained. Finally, we explain evaluation results of three controllers: the controller with both structure and circle adjustment, the controller with only structure adjustment, and the controller without both structure and circle adjustment.

5.1 Adjustment result of controller structure

As a result of applying the adjustment of the controller structure, Basis filter became one notch filter and three phase-lead compensations when $m = 3$ and the parameters were adjusted in Table.3. The pole-zero cancellation

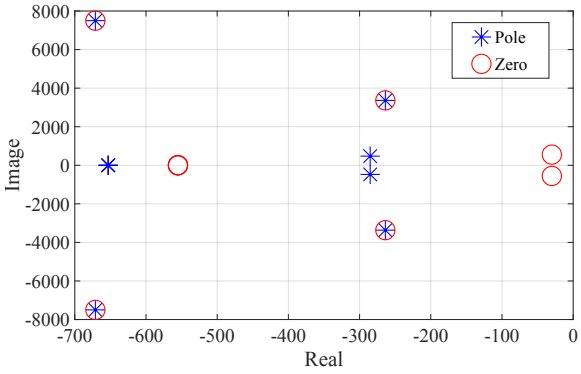

Fig. 7. Pole-zero placement of the Basis filter at the adjustment of controller structure

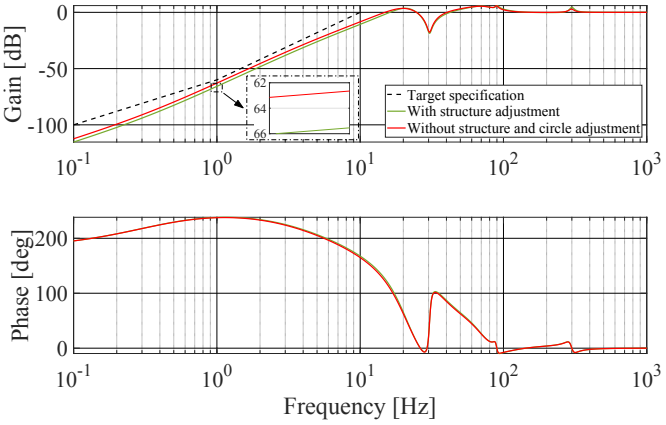

Fig. 8. Comparison for sensitivity function at the adjustment of controller structure

occurred in two notch filter and is confirmed from Fig. 7. The frequency characteristic of Basis filter is shown in Fig.10-(i). Especially, it is possible to confirm that the gain is largely reduced around 90 Hz and the effect of the second vibration mode is to be suppressed. From Fig.8, it can be confirm that the gain of the sensitivity function has decreased by approximately 2 dB.
As a result of the adjustment, the gain margin value and the phase margin value were 6.69 db and 38.5 deg, respectively. Since both margins are 10 % larger than the constraint conditions, we designed the controller with higher disturbance suppression characteristics by adjusting the margins.

5.2 Adjustment result of stability-margin criterion circle

As a result of adjusting the gain margin based on (9), we obtained the gain margin: 6.02 dB and the phase margin: 35.5 deg when $n = 3$ shown in Table.2. From Fig.12, the stability-margin criterion circle moves in the negative direction on the real axis. In addition, as a result of the optimization using the target gain margin and target phase margin, Basis filter became one notch filter and three phase-lead compensations. The frequency characteristic of Basis filter is shown in Fig.10-(ii). Moreover, from Fig.11 it can be confirm that the gain of the sensitivity function has decreased by approximately 2 dB.

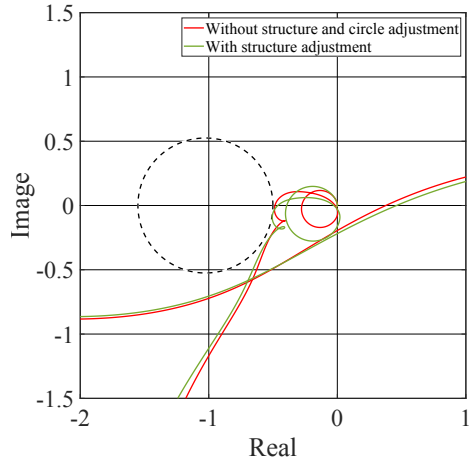

Fig. 9. Comparison for Nyquist diagram at the adjustment of controller structure

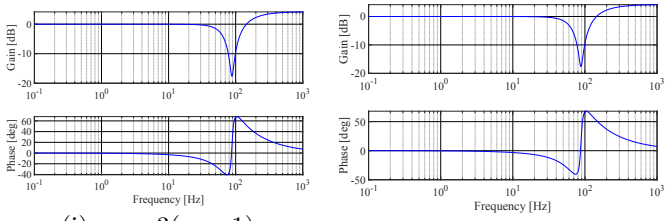

(i) $m = 3(n = 1)$ (ii) $n = 3$

Fig. 10. Frequency response of Basis filter

Table 2. Adjusted result of stability margin

Number of adjustment times : n	1	2	3	Unit
Obtained gain margin : G_m(n)	6.69	5.89	6.02	dB
Target gain margin : G_{obj}(n)	6.00	5.38	5.48	dB
Obtained phase margin	38.5	34.9	35.5	deg
Target phase margin	30.0	30.0	30.0	deg

Table 3. Adjusted parameters of the controller ($m = 1$: without structure and circle adjustment, $n = 1$: with structure adjustment, $n = 3$: with both structure and circle adjustment)

Sym	$m = 1$	$n = 1$	$n = 3$	Unit
K_p	49.6	55.6	60.8	rad/s
K_v	60.6	67.2	70.8	rad/s
K_i	2.99 $\times 10^3$	3.73 $\times 10^3$	4.40 $\times 10^3$	1/s
ω_{f1}	88.3	88.1	88.1	Hz
ζ_{d1}	0.413	0.515	0.517	rad/s
α_1	0.143	0.105	0.105	-
α_2	-	1.00	1.00	-
α_3	-	1.00	1.00	-
$\omega_{\ell 1}$	1.15$\times 10^3$	88.4	88.4	Hz
β_{n1}	0.850	0.850	0.850	-
$\omega_{\ell 2}$	-	88.3	88.4	Hz
β_{n2}	-	0.850	0.850	-
$\omega_{\ell 3}$	-	88.3	88.3	Hz
β_{n3}	-	0.850	0.850	-

5.3 Comparison for disturbance response

We compared the maximum value of the disturbance response shown in Fig.13 when a 1 A current disturbance was applied at t = 0.1. The value of the controller with both structure and circle adjustment is the least (101 µm). The value of the controller without both structure and

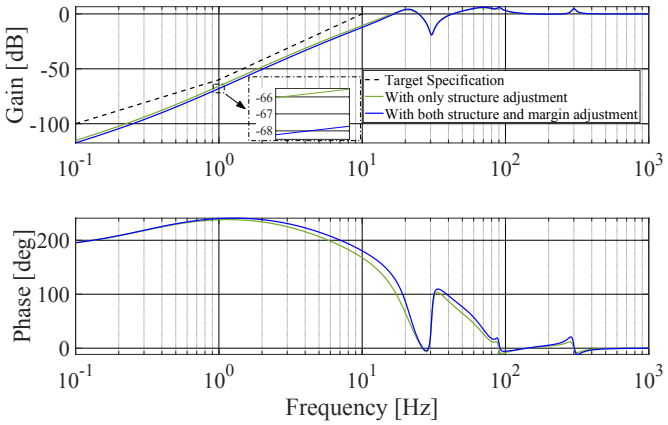

Fig. 11. Comparison for sensitivity function

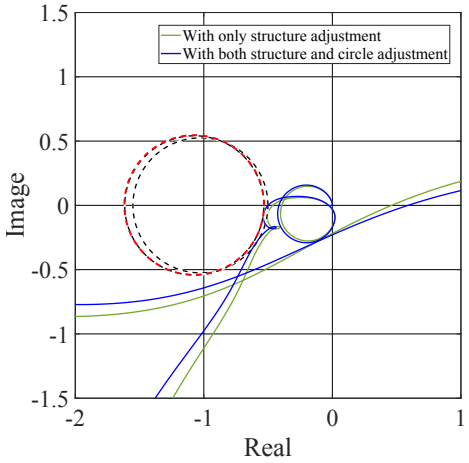

Fig. 12. Comparison for Nyquist diagram

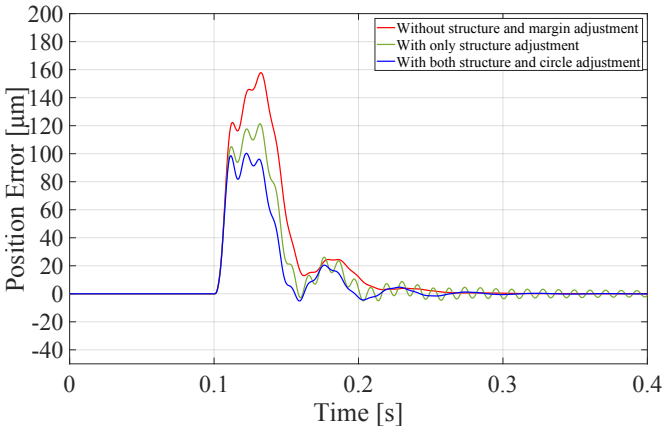

Fig. 13. Comparison for time response of the position error in the simulation

circle adjustment is 158 µm. This result illustrates that the proposed method enables us to design the more improved controller.

6. EXPERIMENT FOR VALIDATION

We evaluated the maximum value of the disturbance response with the single positioning device described in section 4. The evaluation results are shown in Fig.14 and Table.4 as the controller performance.

Table 4. Maximum value of the position error ($m = 1$: without structure and circle adjustment, $n = 1$: with structure adjustment, $n = 3$: with both structure and circle adjustment)

Symbol	$m = 1$	$n = 1$	$n = 3$	Unit
Maximum value (Sim)	158	121	101	µm
Ratio (Sim)	-	23.4	32.3	%
Maximum value (Exp)	162	118	106	µm
Ratio (Exp)	-	27.2	34.6	%

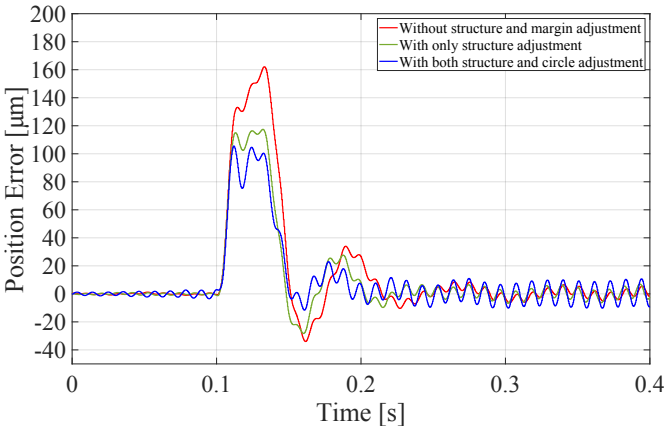

Fig. 14. Comparison for time response of the position error in the experiment

6.1 Condition

We set position reference X_{ref} to 0 and added a 1 A step-like disturbance current d shown Fig.2 to current reference at 0.1 seconds after starting the positioning operation. The position of the carriage was measured by the linear sensor as a position error. Sampling period was set to 40 µs.

6.2 Result

The maximum value of the disturbance response is least on the case of the proposed method (n = 3), which is 106 µm, 34.6% lower than the value without structure and circle adjustment. Moreover, the value of the proposed method is lower than with only structure adjustment. This result illustrates that the proposed method enables us to overcome the conservativeness of the circle condition. The results will help design an improved controller.

7. CONCLUSIONS

In this study, we proposed the automatic adjustment method that enables us to optimize controller parameters, controller structure and to overcome the conservativeness of the stability circle in the cascade control system. The effectiveness of the proposed method was verified by the positioning operation with the precise positioning device. However, the residual oscillation occured after the positioning. We think that the modeling error of the second vibration mode caused this oscillation because the power spectrum of the FFT analysis is large at the frequency of the second vibration mode (89 Hz). We plan to study a system identification method to gain a more accurate model of the plant.

REFERENCES

Apkarian, P. and Noll, D. (2006). Nonsmooth H∞ Synthesis. *IEEE Transactions on Automatic Control*, 51(1), 71–86.

Apkarian, P. and Noll, D. (2017). The H∞ Control Problem is Solved. *AerospaceLab Journal*, (13), 1–11.

Do, T.M.T. and Artieres, T. (2012). Regularized bundle methods for convex and non-convex risks. *The Journal of Machine Learning Research*, 13, 3539–3583.

Fujimoto, H. and Sakata, K. (2014). Multirate pwm control of precision stage for ultrahigh-speed nanoscale positioning. *IEEJ Journal of Industry Applications*, 3(3), 270–276.

Gahinet, P. and Apkarian, P. (2011). Decentralized and fixed-structure h∞ control in matlab. In *2011 50th IEEE Conference on Decision and Control and European Control Conference*, 8205–8210.

Karimi, A., Galdos, G., and Longchamp, R. (2008). Robust fixed-order h∞ controller design for spectral models by convex optimization. In *2008 47th IEEE Conference on Decision and Control*, 921–926.

Kitayoshi, R. and Fujimoto, H. (2019). Automatic adjustment method of controller structure and parameter based on structured h∞control. In *IECON 2019 - 45th Annual Conference of the IEEE Industrial Electronics Society*, volume 1, 3263–3268.

Maeda, Y., Kuroda, E., Uchizono, T., and Iwasaki, M. (2018). Hybrid optimization method for high-performance cascade structure feedback controller design. In *IECON 2018 - 44th Annual Conference of the IEEE Industrial Electronics Society*, 4588–4593.

Molander, P. and Willems, J. (1980). Synthesis of state feedback control laws with a specified gain and phase margin. *IEEE Transactions on Automatic Control*, 25(5), 928–931.

Nakamura, K., Yubai, K., Yashiro, D., and Komada, S. (2016). Controller design method achieving maximization of control bandwidth by using nyquist diagram. In *2016 International Automatic Control Conference (CACS)*, 35–40.

Ohnishi, W. (2019). Frequency response data-based feedback controller auto-tuning method utilizing both collocated and non-collocated sensors. *IEEJ Transactions on Industry Applications*, 139(11), 924–932.

Oomen, T. (2018). Advanced motion control for precision mechatronics: Control, identification, and learning of complex systems. *IEEJ Journal of Industry Applications*, 7(2), 127–140.

Seki, K., Noda, D., and Iwasaki, M. (2018). Dual-loop controller design considering robust vibration suppression in piezo-actuated stage systems. *IEEJ Journal of Industry Applications*, 7(6), 488–494.

Yuille, A.L. and Rangarajan, A. (2003). The Concave-Convex Procedure. *Neural Computation*, 15(4), 915–936.

Zames, G. (1966). On the input-output stability of time-varying nonlinear feedback systems–Part II: Conditions involving circles in the frequency plane and sector nonlinearities. *IEEE Transactions on Automatic Control*, 11(3), 465–476.